Supplementary Information

Comparative study of Ir(III) complexes with pyrazino[2,3-f][1,10]phenanthroline and pyrazino[2,3-f][4,7]phenanthroline ligands in light-emitting electrochemical cells (LECs)

Iván González,[a] Paulina Dreyse,[b] Diego Cortés-Arriagada,[c]MaheshSundararajan,[d] ClaudioMorgado,[b] Iván Brito,[e] Cristina Roldán-Carmona,[f]Henk J. Bolink,[f]and Bárbara Loeb[a]

[a]*Departamento de Química Inorgánica,Facultad de Química, Pontificia Universidad Católica de Chile, Av. Vicuña Mackenna 4860, Macul, Santiago, Chile. E-mail: ilgonzalez@uc.cl*

[b]*Departamento de Química, Universidad Técnica Federico Santa María, Av. España 1680, Valparaíso, Chile. E-mail: paulina.dreyse@usm.cl*

[c] *Nucleus Millennium ChemicalProcesses and Catalysis, Laboratorio de Química Teórica Computacional,Departamento de Química-Teórica,Facultad de Química, Pontificia Universidad Católica de Chile, Av. Vicuña Mackenna 4860, Macul, Santiago, Chile.*

[d]*Theoretical Chemistry Section, Bhabha Atomic Research Centre, Mumbai – 400 085, India, E-mail: smahesh@barc.gov.in*

[e]*Departamento de Química, Universidad de Antofagasta, Av. Angamos 601, Antofagasta, Chile.*

[f]*Instituto de Ciencia Molecular, Universidad de Valencia, 46980 Paterna, Spain. E-mail: henk.bolink@uv.es*

^{1}H NMR Characterization

The ^{1}H NMR spectra of the complexes $[Ir(F_2ppy)_2(ppl)][PF_6]$ and $[Ir(F_2ppy)_2(ppz)][PF_6]$ are shown below. The labels used in the following scheme (Fig. 1 in the main text) have been employed in the analysis of the ^{1}H NMR spectra.

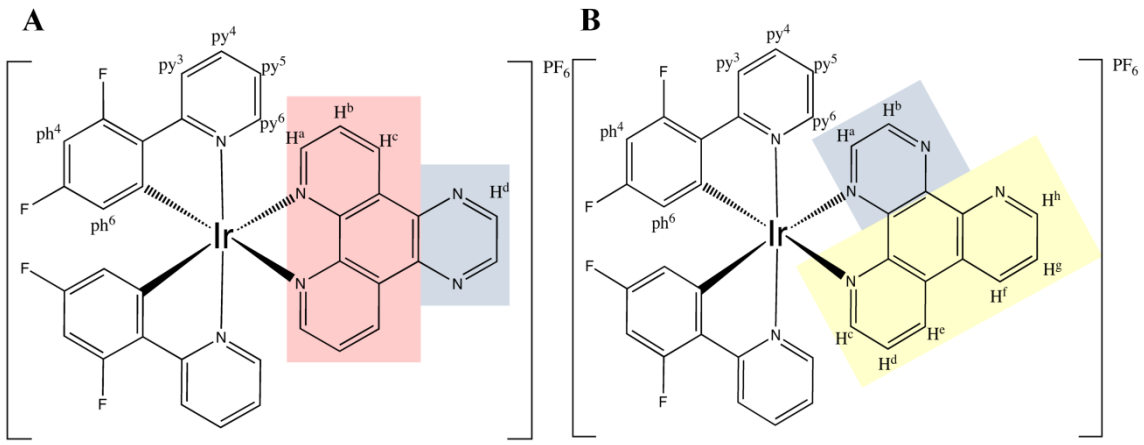

*Chemical structures of $[Ir(F_2ppy)_2(ppl)][PF_6]$ (**A**) and $[Ir(F_2ppy)_2(ppl)][PF_6]$ (**B**) complexes. Labeling of protons used for ^{1}H NMR analysis.*

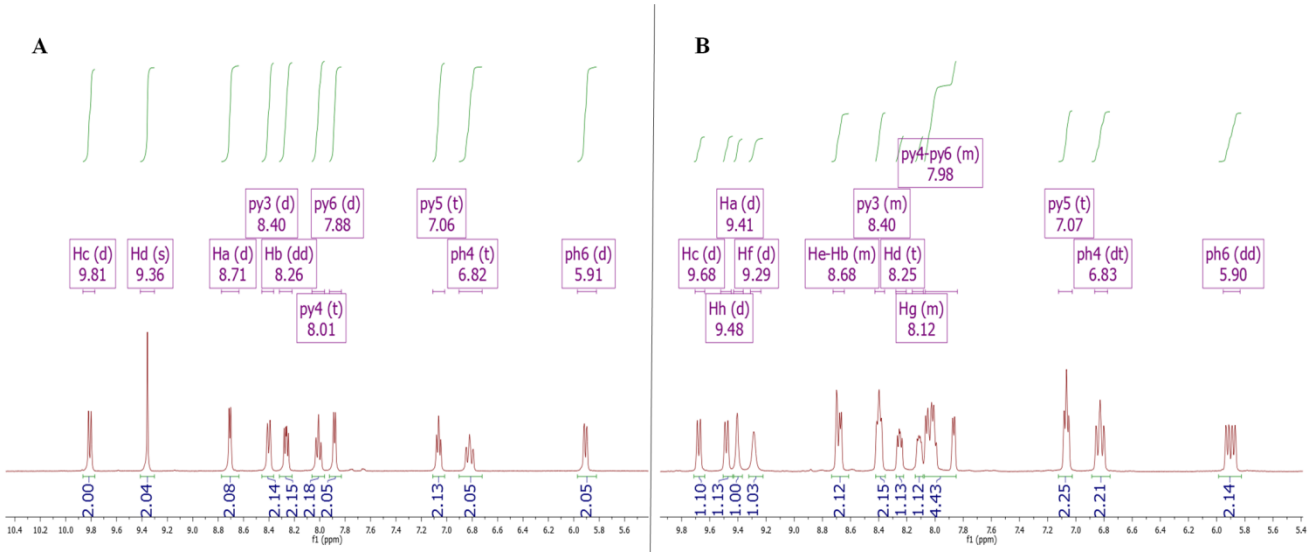

Figure S1. *Down field region(**A**) ^{1}H-NMR spectrum of $[Ir(F_2ppy)_2(ppl)][PF_6]$ and (**B**) $[Ir(F_2ppy)_2(ppz)][PF_6]$ (400 MHz, $(CD_3)_2CO$)).*

X-ray crystallography characterization

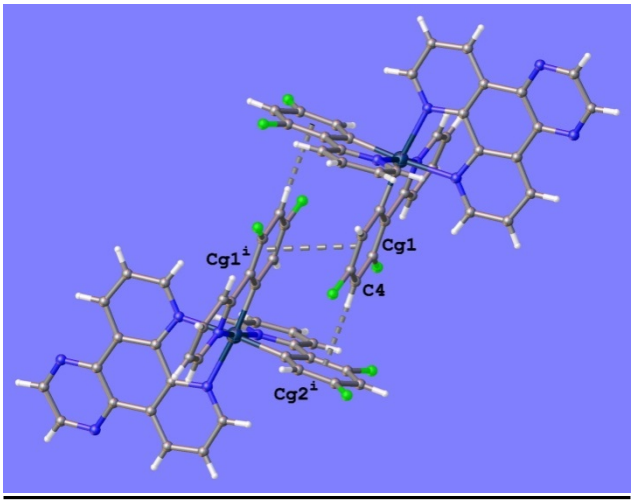

Figure S2. *$\pi-\pi$ stacking interactions of $[Ir(F_2ppy)_2(ppl)][PF_6]$ complex.*

Extra theoretical data

Singlet/triplet molecular structures

The optimized structures were very close to the corresponding experimental X-ray structure. Following the nomenclature used in the X-ray section, the bond lengths for both Ir-N and Ir-C, for ancillary and cyclometalated ligands were reproduced. In both complexes, the Ir-C bond lengths are shorter compared to Ir-N, for example: Ir-C_{61} (F_2ppy) = 2.017 Å v/s Ir-N_1(ppl) = 2.182 Å, in $[Ir(F_2ppy)_2(ppl)][PF_6]$ and Ir-C_{61} (F_2ppy) = 2.019 Å v/s Ir-N_1 (ppz) = 2.188 Å in $[Ir(F_2ppy)_2(ppz)][PF_6]$. At the T_1 equilibrium geometry, the Ir-ligand bond lengths (where ligand is F_2ppy, ppl, or ppz) are slightly reduced with respect to the ground state geometry of both complexes (Table S1). For instance, in the $[Ir(F_2ppy)_2(ppl)]^+$ complex, the Ir-N_{ppl}, Ir-$N_{F2\text{-}ppy}$, and Ir-C_{ppy} distances are reduced 0.029, 0.006 and 0.011 Å, respectively; in the same way, for the $[Ir(F_2ppy)_2(ppz)]^+$ complex, the Ir-N_{ppz}, Ir-$N_{F2\text{-}ppy}$, and Ir-C_{ppy} distances are reduced at least 0.007, 0.005 and 0.009 Å, respectively.

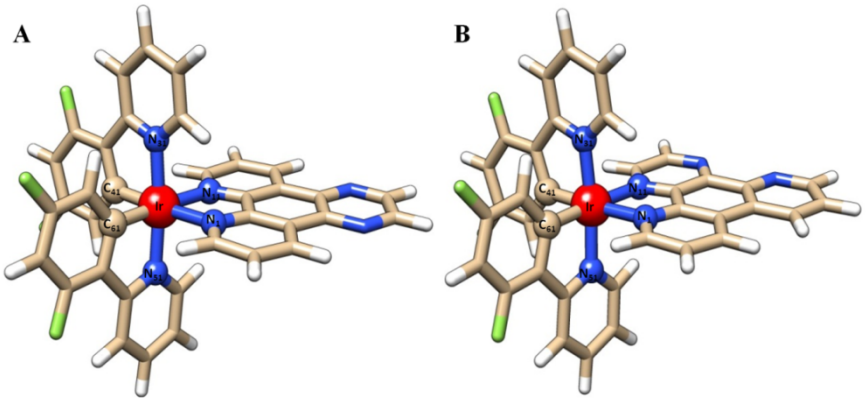

Figure S3. *Groundsingletstate (S_0) optimizedstructures of A) $[Ir(F_2ppy)_2(ppl)]^+$ and B) $[Ir(F_2ppy)_2(ppz)]^+$complexes.*

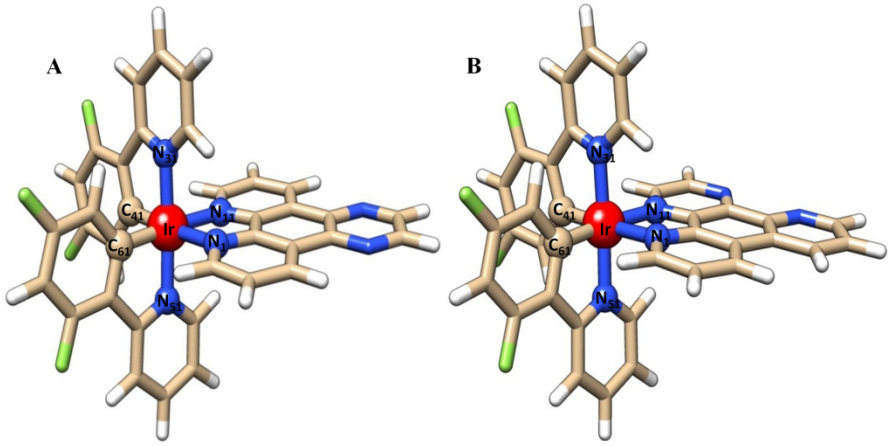

Figure S4. *First triplet state (T_1) optimized structures of A) $[Ir(F_2ppy)_2(ppl)]^+$ and B) $[Ir(F_2ppy)_2(ppz)]^+$ complexes.*

Table S1. *Optimized structural parameters in angstroms (Å) (more experimental from X-ray data) of S_0 and T_1 states of $[Ir(F_2ppy)_2(ppl)]^+$ and $[Ir(F_2ppy)_2(ppz)]^+$ complexes.*

	$[Ir(F_2ppy)_2(ppl)]^+$		$[Ir(F_2ppy)_2(ppz)]^+$	
	S_0	T_1	S_0	T_1
$Ir\text{-}N_1$	2.182 (2.146)	2.153	2.188 (2.147)	2.181
$Ir\text{-}N_{11}$	2.182 (2.136)	2.153	2.167 (2.148)	2.132
$Ir\text{-}N_{31}$	2.066 (2.047)	2.060	2.068 (2.030)	2.063
$Ir\text{-}N_{51}$	2.066 (2.047)	2.060	2.068 (2.040)	2.061
$Ir\text{-}C_{41}$	2.017 (1.997)	2.006	2.017 (2.005)	1.995
$Ir\text{-}C_{61}$	2.017 (2.008)	2.006	2.019 (2.005)	2.010

Frontier Kohn-Sham orbitals

Considering literature information for related Ir(III) complexes, where the allowed singlet transition take place from the HOMO-N manifold to the LUMO+N manifold, these molecular orbitals were analyzed. The last five HOMO are mainly non-bonding orbitals localized in the $[Ir(F_2ppy)_2]^+$ fragment, denoting its donor character. HOMO-1, HOMO-2 and HOMO-3 are mainly positioned on the F_2ppy based ligands with some of the Ir_dcharacter, while HOMO-5 and HOMO-4 (below ~1 eV from the HOMO) are metal centered. On the other hand, the first three closely spaced low lying unoccupied MOs are due to acceptor π* orbitals delocalized at the ancillary ligand. Note that in the $[Ir(F_2ppy)_2(ppl)]^+$ complex, the delocalization of LUMO, LUMO+1 and LUMO+2 take place mainly on the phenanthroline fragment, pyrazine fragment, and all the ligand, respectively, while for $[Ir(F_2ppy)_2(ppz)]^+$, delocalization takes place on the pyrazine fragment, all the ligand, and phenanthroline moiety, respectively. Besides, the electron withdrawing nature of the ppz ligand compared to ppl results in somewhat stabilized HOMO-LUMO orbitals for the $[Ir(F_2ppy)_2(ppz)]^+$ complex, as predicted from the electrochemical and photophysical experimental measurements. Note that the computed HOMO-LUMO energy gap are 3.05 eV and 2.90 eV for $[Ir(F_2ppy)_2(ppl)]^+$and $[Ir(F_2ppy)_2(ppz)]^+$ complexes, respectively. These findings are in agreement with ΔE values calculated from the data of the electrochemical section (2.84 V and 2.66 V for $[Ir(F_2ppy)_2(ppl)][PF_6]$ and $[Ir(F_2ppy)_2(ppz)][PF_6]$ complexes, respectively).

Singlet-Singlet excited states

The nature of transitions is listed in Table S2. In the $[Ir(F_2ppy)_2(ppl)]^+$ complex, the ^{1}MLCT band is composed by medium intense transitions at 381 (S_7), 379 (S_9) and 378 nm (S_{10}). Figure 7 show that transitions at 381 and 378 nm involve electron promotion from metal and F_2ppy-π orbitals to pplπ* orbitals. Therefore, the broad band experimentally observed must be correctly assigned as ^{1}MLCT + ^{1}LLCT; in addition, transition at 379 is observed as ^{1}MLCT+^{1}ILCT (intraligand charge transfer), involving only the F_2ppy ligand. Likewise, in the $[Ir(F_2ppy)_2(ppz)]^+$ complex, the ^{1}MLCT transitions (including ^{1}LLCT character) appear at 383 (S_8) and 374 nm (S_{11}); ^{1}LLCT transition is observed at 397 nm due to the S_6 state, with electron promotion from F_2ppy ligand toward ppz ligand. Besides, S_{10} state at 376 nm shows a ^{1}ILCT character and some of ^{1}MLCT, where electron is promoted to F_2ppy ligand. On the other hand, the most intense bands due to π→π* transitions appear at 262 and 263 nm for the $[Ir(F_2ppy)_2(ppl)]^+$ complex, and at 277 nm for $[Ir(F_2ppy)_2(ppz)]^+$, in good agreement with the experimental absorption spectrum. Moreover, both experimental and theoretical results show that there is not a meaningful difference in the UV-Vis spectra of $[Ir(F_2ppy)_2(ppl)]^+$ and $[Ir(F_2ppy)_2(ppz)]^+$.

Table S2. *Excitation energies of singlet excited states in nm, oscillator strengths (f), and nature of electron transitions including the monoexitations and its percentage of contribution. H and L stand for HOMO and LUMO, respectively.*

a) $[Ir(F_2ppy)_2(ppl)]^+$

Energy (nm)	*f*	PercentageContribution	Monoexcitations	Transitionassignment
381.0	0.035	19% 30% 15% 28%	H-5 → L H-3 → L H-2 → L+2 H-1 → L+1	$Ir_d \rightarrow ppl_{\pi^*}$ $Fppy_{\pi} + Ir_d \rightarrow ppl_{\pi^*}$ $Fppy_{\pi} + Ir_d \rightarrow ppl_{\pi^*}$ $Fppy_{\pi} + Ir_d \rightarrow ppl_{\pi^*}$
378.9	0.028	25% 69%	H-1 → L+2 H → L+3	$Fppy_{\pi} + Ir_d \rightarrow ppl_{\pi^*}$ $Ir_d + Fppy_{\pi} \rightarrow Fppy_{\pi^*}$
377.7	0.023	35% 52%	H-3 → L H-1 → L+1	$Fppy_{\pi} \rightarrow ppl_{\pi^*}$ $Fppy_{\pi} + Ir_d \rightarrow ppl_{\pi^*}$
349.7	0.032	60% 19%	H-4 → L+2 H-3 → L+1	$Ir_d \rightarrow ppl_{\pi^*}$ $Fppy_{\pi} \rightarrow ppl_{\pi^*}$
343.5	0.037	19% 69%	H-4 → L+2 H-3 → L+1	$Ir_d \rightarrow ppl_{\pi^*}$ $Fppy_{\pi} \rightarrow ppl_{\pi^*}$
309.7	0.052	14% 67%	H-4 → L+3 H-1 → L+4	$Ir_d \rightarrow Fppy_{\pi^*}$ $Fppy_{\pi} + Ir_d \rightarrow Fppy_{\pi^*}$
302.6	0.030	22% 35% 14% 20%	H-5 → L+4 H-4 → L+3 H-3 → L+4 H-2→ L+3	$Ir_d \rightarrow Fppy_{\pi^*}$ $Ir_d \rightarrow Fppy_{\pi^*}$ $Fppy_{\pi} \rightarrow Fppy_{\pi^*}$ $Fppy_{\pi} + Ir_d \rightarrow Fppy_{\pi^*}$
300.5	0.058	15% 29% 30%	H-4 → L+4 H-3 → L+3 H-2 → L+4	$Ir_d \rightarrow Fppy_{\pi^*}$ $Fppy_{\pi} \rightarrow Fppy_{\pi^*}$ $Fppy_{\pi} + Ir_d \rightarrow Fppy_{\pi^*}$
295.2	0.081	15% 73%	H-4 → L+3 H-3 → L+4	$Ir_d \rightarrow Fppy_{\pi^*}$ $Fppy_{\pi} \rightarrow Fppy_{\pi^*}$
290.2	0.044	55% 14%	H-5 → L+4 H-2 → L+5	$Ir_d \rightarrow Fppy_{\pi^*}$ $Fppy_{\pi} + Ir_d \rightarrow Fppy_{\pi^*}$
262.7	0.105	73%	H-4 → L+5	$Ir_d \rightarrow Fppy_{\pi^*}$
261.5	0.271	10% 10% 27% 24%	H-4 → L+5 H-2 → L+5 H-1 → L+6 H → L+9	$Ir_d \rightarrow Fppy_{\pi^*}$ $Fppy_{\pi} + Ir_d \rightarrow Fppy_{\pi^*}$ $Fppy_{\pi} + Ir_d \rightarrow Fppy_{\pi^*}$ $Ir_d + Fppy_{\pi} \rightarrow Fppy_{\pi^*}$

b) $[Ir(F_2ppy)_2(ppz)]^+$

Energy (nm)	*f*	PercentageContribution	Monoexcitations	Transitionassignment
397.2	0.001	95%	H-3→L	$Fppy_{\pi}$→ ppz_{π^*}
383.3	0.055	51% 10% 32%	H-5→L H-4→ L+1 H-2 → L+1	Ir_d→ ppz_{π^*} Ir_d→ ppz_{π^*} $Fppy_{\pi}$ + Ir_d→ ppz_{π^*}
376.0	0.036	95%	H→L+3	Ir_d + $Fppy_{\pi}$→ $Fppy_{\pi^*}$
374.4	0.035	30% 63%	H-5→ L H-2→ L+1	Ir_d→ ppl_{π}→ ppz_{π^*} $Fppy_{\pi}$ + Ir_d→ ppz_{π^*}
346.6	0.084	66% 11%	H-4→L+1 H-3→L+1	Ir_d→ ppl_{π^*}→ ppz_{π^*} $Fppy_{\pi}$→ ppl_{π^*}
308.1	0.069	10% 11% 34%	H-7→L+1 H-4→L+3 H-1→ L+4	ppz_{π}→ ppz_{π^*} Ir_d→$Fppy_{\pi^*}$ $Fppy_{\pi}$→ $Fppy_{\pi^*}$
307.2	0.046	12% 39% 12% 15%	H-3 → L+3 H-2 → L+4 H-1 → L+3 H → L+6	$Fppy_{\pi}$→ $Fppy_{\pi^*}$ $Fppy_{\pi}$ + Ir_d→ $Fppy_{\pi^*}$ $Fppy_{\pi}$→ $Fppy_{\pi^*}$ Ir_d + $Fppy_{\pi}$→ $Fppy_{\pi^*}$
299.8	0.045	19% 39% 15%	H-5 → L+4 H-4 → L+3 H-2 → L+3	Ir_d→ $Fppy_{\pi^*}$ Ir_d→ $Fppy_{\pi^*}$ $Fppy_{\pi}$ + Ir_d→
298.3	0.042	53% 18%	H-3 → L+3 H-2 → L+4	$Fppy_{\pi}$→ $Fppy_{\pi^*}$ $Fppy_{\pi}$ + Ir_d→
293.9	0.033	26% 57%	H-9 → L+1 H-3 → L+4	ppz_{π} + $Fppy_{\pi}$→ppz_{π^*} $Fppy_{\pi}$→ $Fppy_{\pi^*}$
286.6	0.039	40%	H-5 → L+4	Ir_d→ $Fppy_{\pi^*}$
277.4	0.161	17% 14% 40%	H-8 → L H-8 → L+2 H-7 → L+1	ppz_{π}→ ppz_{π^*} ppz_{π}→ ppz_{π^*} ppz_{π}→ ppz_{π^*}
261.3	0.031	62%	H-3 → L+5	$Fppy_{\pi}$→ $Fppy_{\pi^*}$

Triplet excited state calculations

In order to characterize the emissive state of interest for LEC applications, firstly the lowest spin forbidden transitions to the triplet excited states due to vertical transitions from the S_0 ground state were analyzed. The first triplet (T_1) state appears at 527 and 572 nm for $[Ir(F_2ppy)_2(ppl)]^+$ and $[Ir(F_2ppy)_2(ppz)]^+$ respectively, close at its respective S_1 states. T_1 shows to be a mixture of ^{3}MLCT and ^{3}LLCT transitions involving the HOMO and LUMO orbitals. The next high lying triplets (T_2 and T_3) appear with a shift of at least 71.4 nm from the T_1 state: for $[Ir(F_2ppy)_2(ppl)]^+$, T_2 and T_3 states appear at 456 and 448 nm, respectively; while for $[Ir(F_2ppy)_2(ppz)]^+$ these states appear at 461 and 457 nm (2.71 eV), respectively. Given that the calculated energy for the vertical excitation to the T_1 state is close to experimental emission, and markedly shifted from T_1 for others triplets, emission would occurs only from the T_1 state. These transitions are shown in Table S3.

Table S3.*Excitation energies of triplet states in nm (with excited states in parenthesis) and nature of electron transitions (including the monoexitations and its percentage of contribution). H and L stand for HOMO and LUMO, respectively.*

a) $[Ir(F_2ppy)_2(ppl)]^+$

Energy (nm)	PercentageContribution	Monoexcitations	Transitionassignment
527.0 (T_1)	92%	H → L	$Fppy_{\pi} + Ir_d \rightarrow ppl_{\pi^*}$
455.6 (T_2)	96%	H → L+2	$Fppy_{\pi} + Ir_d \rightarrow ppl_{\pi^*}$
447.9 (T_3)	92%	H → L+1	$Fppy_{\pi} + Ir_d \rightarrow ppl_{\pi^*}$
429.9 (T_4)	40% 47%	H-4 → L H-2 → L	$Ir_d \rightarrow ppl_{\pi^*}$ $Fppy_{\pi} \rightarrow ppl_{\pi^*}$

b) $[Ir(F_2ppy)_2(ppz)]^+$

Energy (nm)	PercentageContribution	Monoexcitations	Transitionassignment
571.5	97%	H → L	$Fppy_{\pi} + Ir_d \rightarrow ppz_{\pi^*}$
461.3	32% 51%	H-1→L H→ L+1	$Fppy_{\pi} \rightarrow ppz_{\pi^*}$ $Fppy_{\pi} + Ir_d \rightarrow ppz_{\pi^*}$
457.1	22% 38% 21%	H-4 →L H-2→L H→ L+1	$Ir_d \rightarrow ppz_{\pi^*}$ $Fppy_{\pi} + Ir_d \rightarrow ppz_{\pi^*}$ $Fppy_{\pi} + Ir_d \rightarrow ppz_{\pi^*}$
453.6	16% 18% 31% 24%	H-4→ L H-2→ L H-1→ L H→ L+1	$Ir_d \rightarrow ppz_{\pi^*}$ $Fppy_{\pi} + Ir_d \rightarrow ppz_{\pi^*}$ $Fppy_{\pi} + Ir_d \rightarrow ppz_{\pi^*}$ $Fppy_{\pi} + Ir_d \rightarrow ppz_{\pi^*}$